Full State Estimation for Helicopter Slung Load System

Bisgaard, Morten; la Cour-Harbo, Anders; Bendtsen, Jan Dimon

Publication date:
2007

Document Version
Publisher's PDF, also known as Version of record

Full State Estimation for Helicopter Slung Load System

Morten Bisgaard*, Anders la Cour-Harbo† and Jan Dimon Bendtsen†

Aalborg University, Department of Electronic Systems, Section for Control and Automation, Denmark

This paper presents the design of a state estimator system for a generic helicopter based slung load system. The estimator is designed to deliver full rigid body state information for both helicopter and load and is based on the unscented Kalman filter. Two different approaches are investigated: One based on a parameter free kinematic model and one based on a full aerodynamic helicopter and slung load model. The kinematic model approach uses acceleration and rate information from two Inertial Measurement Units, one on the helicopter and one on the load, to drive a simple kinematic model. A simple and effective virtual sensor method is developed to maintain the constraints imposed by the wires in the system. The full model based approach uses a complex aerodynamical model to describe the helicopter together with a generic rigid body model. This rigid body model is based on a redundant coordinate formulation and can be used to model all body to body slung load suspension systems. Both estimators include bias estimation for the accelerometers and gyros and the model based estimator furthermore includes estimation of external wind disturbances. A vision system is used to measure the motion of the load relative to the helicopter. A method is devised to reduce the execution time of the process model in the unscented Kalman filter. The two approaches are tested through simulation and compared. The full model based approach shows better results than the kinematic model aproach, but at the cost of a larger computational burden.

I. Introduction

Helicopters carrying slung loads are widely used for a number of applications such as firefighting and cargo transport, and such systems have been studied extensively through the last decades. However, almost all this research has been focused on stability analysis and design of stability augmenting controllers to aid pilots in the handling of slung loads, see for instance [1] and [2]. The design of an autonomous Unmanned Aerial Vehicle (UAV) carrying slung loads is an almost untouched subject in the literature. The contribution of this paper is the development of a vision based state estimator using an unscented Kalman filter approach to estimate the rigid body states of helicopter and slung load concurrently. Two estimators are investigated: A Inertial Measurement Unit (IMU) driven filter that includes IMU bias estimation, and a full model based filter that uses a full dynamic helicopter and slung load model, and includes estimation of IMU bias and external wind disturbances. A vision system is used to measure the position and attitude of the load.

The motivation for this study is its intended use with a small-scale helicopter in a landmine detection application. The global landmine problem is indeed significant, with the United Nations estimating that there are more than 100 million mines in the ground and that 50 people are killed each day by mines worldwide[3]. The idea is to suspend the mine detection equipment as a slung load underneath a low-cost model helicopter, which has the considerable advantage over a ground based vehicle that it needs no contact with the ground; there is no risk of the mines being detonated in the detection process and the helicopter is independent of the type of terrain it operates in. The objective is to give the system a certain level of autonomy such that it will be capable of searching specific areas for mines by itself and thus requiring no helicopter pilot skills of the operating crew.

*Phd Student, Department of Electronic Systems, Section for Control and Automation, Fredrik Bajers Vej 7C DK-9220 Aalborg East, Denmark.

†Associate Professor, Department of Electronic Systems, Section for Control and Automation, Fredrik Bajers Vej 7C DK-9220 Aalborg East, Denmark.

This paper will begin by describing the helicopter and slung load system that is used in this research. Then a discussion of previous work is given and the vision algorithms are presented. The unscented Kalman filter is briefly presented and then the development of the two estimators are described. Finally, the estimators are tested and compared to each other.

I.A. System Description

An important difference between the mine detection application discussed above and more traditional slung load applications like general cargo transport is that the mine detection requires a suspension system that gives control on the yaw angle of the load. This means that, whereas for general cargo transport the most common suspension types are 1 (a) and (d), the types used in the mine detection application will be types like 1 (b) or (c). These types of suspension couple the yaw motion of the helicopter to the yaw motion of the load.

(a) (b) (c) (d)

Figure 1. Four different slung load configurations. Single wire (a), Dual wire (b), Inverted V (c), Four wire centred (d).

Here the estimators are developed for a modified Bergen Industrial Twin (see figure 2) equipped with appropriate sensors. It has a stand alone Novatel GPS receiver using EGNOS, a HMR2300 magnetometer, a Falcon GX IMU, a tachometer to measure the engine RPM, and a camera used to determine the load position and yaw angle relative to the helicopter. The load is equipped with another Falcon GX IMU. All the sensors are interfaced to the 1.8 GHz on-board laptop computer. The helicopter is capable of carrying slung loads of up to 4 kg using either one or two suspension points.

Figure 2. The modified Bergen Industrial Twin

II. Previous Work

State estimators and sensor fusion algorithms for autonomous helicopters have been the subject of quite some research for the past two decades, but with respect to slung load systems there are almost no previous published results. For helicopter state estimation, a number of different approaches have been tried over the years, using both kinematic model and full model based methods. However, most work has been based on a kinematic model approach as helicopter models are often highly non-linear, quite complex to work with, and have rather high computational requirements.

In [4] position, velocity, and attitude determination is demonstrated using a four antenna carrier-phase differential GPS (CDGPS) setup. The very high accuracy of the CDGPS made it possible to achieve position estimates with an accuracy of 3 cm and attitude estimates with an accuracy of a couple of degrees.

A system for estimating attitude based on rate gyros and inclinometers fused through a complementary filter is demonstrated in [5]. With the complementary filter, which fuses high bandwidth information from the gyros with low bandwidth information from the inclinometers, attitude accuracy of a couple of degrees is achieved. Another kinematic model approach is given in [6], which describes the use of a Kalman filter driven by accelerations and rates measured by an IMU along with data from GPS and compass as sensor inputs. The idea is to use a simple kinematic model driven by the measured rates for attitude estimation and a simple rigid body dynamic model driven by the measured accelerations for position and velocity estimation. Similar approaches are discussed in [7] and [8], where gyro bias estimation is added to the Kalman filter.

Custom attitude estimation algorithms developed for sparse resource systems are presented in [9], where acceleration and magnetic field measurements are fused to yield an attitude prediction, a CDGPS is used to adjust for dynamic accelerations and rate gyros are used for state updates. Further, it is demonstrated that the custom algorithms shows accuracies comparable with those of a standard EKF setup, but using less computations. In recent years a new type of nonlinear estimator, known as the Unscented Kalman Filter (UKF), has become increasingly popular. In [10] the UKF is used in an IMU driven setup with GPS and barometric data as sensor inputs and it is found to exhibit superior accuracy compared to traditional EKF solutions. In [11] the GPS system is replaced with a triangulation system based on visual cameras, which fused with IMU measurements yields position estimates usable in closed loop.

However, while it is clear that a lot of research has gone into state estimation in helicopter UAV systems, the published work on state estimation in slung load systems is very sparse. To the best of the authors' knowledge, the only publication that even considers the need for state estimation for slung loads is [12]. It discusses a hover control system for a helicopter with a slung load and suggests using an attitude measurement, the angles of a measurement cable from the helicopter to the ground and the angles of the suspension cable as sensor input to a linear Kalman filter.

III. Vision System

The vision system is a digital camera mounted on the helicopter frame and it is looking down on the load. The resulting image is a top-down view of the load and the ground below. To easily identify the load amongst other objects that might appear in the camera view the load is fitted with a visual marker; in this case a white disk on a dark background with a straight line protruding from it. The location of the marker in the image is thus an estimate of the position of the load relative to the helicopter.

To identify the marker in the image two circular Hough transforms with different radii are used. A circular Hough transform maps a 2D data set into another 2D data set such that complete circles are mapped to single points. Since points can be found easily by, for instance, thresholding, it makes the search for circles much simpler. The first of the two transforms uses a radius slightly smaller than the white disk marker and triggers on white. The second transform uses a radius slightly bigger than the white disk marker and triggers on black. Correlating the two transforms triggers only those areas where a sufficiently large round white area is present and surrounded by a dark area. In most scenarios this is sufficient to ensure a stable estimate of the marker location. In fact as long as the image of the marker is fairly good, i.e. not distorted by helicopter vibration, this method produces a sub-pixel precision estimate of the marker location. An illustration of the Hough transform at work is shown in figure 3, where a cicular white slung load is located.

Figure 3. Left: Input to the Hough transform with the located load indicated by a circle. Right: Output of the Hough transform.

It is important to keep the delay in the vision system low and this is ensured by using the previous estimate of the location to choose a subset of the image for analysis in the next image frame (only relevant

when using a camera with a large field of view) and using a threshold to simply ignore the pixels that are too far from white to be the marker.

The measurement is checked for a false detection by examining the pixel detected as the centre of the disk. If it is not sufficiently white, it is assumed that the algorithm has made a false detection and the measurement is discarded. This could happen if the load is outside the field of view (FOV) of the camera. Note that the camera is fixed to the helicopter which means that both load swing and helicopter roll and pitch can result in the load disappearing from the FOV.

When the vision algorithm has detected the pixel position of the load this measurement must be mapped to a 3D load position. This is done by first transforming the pixel position into two angles – a vertical (θ_p) and a horizontal (ϕ_p) – as shown in figure 4. The camera coordinate system is defined to coincide with the helicopter coordinate system when the camera is pointing forward, i.e. the x-axis is pointing in the image direction.

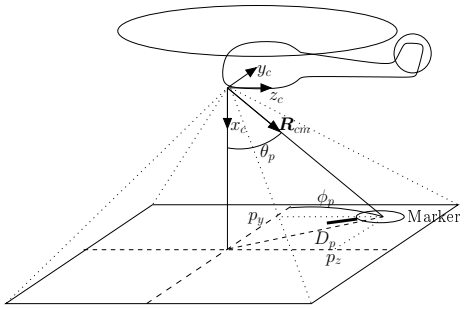

Figure 4. The map of 2D image position to the 3D spatial location.

This is done by assuming that the angle from the camera to the load (θ_p) is proportional to the pixel distance from the load to the image centre. The distance from the image centre to the load is found as

$$D_p = \sqrt{p_y^2 + p_z^2}\,. \tag{1}$$

The angle to the load can then be found as

$$\theta_p = \frac{\alpha_{FOV}}{P_{FOV}} D_p\,, \tag{2}$$

where α_{FOV} is the field of view angle of the camera and P_{FOV} is the number of pixels related to the α_{FOV}. The horizontal angle can be found simply by the relationship between the x and the y pixel position

$$\phi_p = \arctan(p_z,\ p_y)\,. \tag{3}$$

The unit vector from the camera to the load can then be found in the camera coordinate system and rotated into the helicopter coordinate system

$${}^h\boldsymbol{R}_{cl} = \boldsymbol{T}_{hc} \begin{bmatrix} \cos(\theta_p) \\ \sin(\theta_p)\cos(\phi_p) \\ \sin(\theta_p)\sin(\phi_p) \end{bmatrix} \tag{4}$$

where $\boldsymbol{T}_{hc}$ is the direct cosine matrix between the camera and the helicopter.

In order to determine the orientation of the slung load (ψ_{cam}) a straight line is added to the circular marker. This line extends from the centre of the disk and is slightly longer than radius of the disk, thus giving the disk a little 'pin' as shown in figure 5. Once the centre of the marker is found, an angular search is performed in the image to find the direction of the pin. Since the marker background is black and the marker and pin is white, a simple pixel search will suffice. For subpixel accuracy several circles with radii slightly larger than the marker is traced, and the resulting arrays of pixel values are approximated with splines or Gaussian functions to find an extremal value (the color white) indicating the direction of the marker. This approach is fast and transparent to small changes in roll and pitch of the load. Note that the straight line should be relatively thin, otherwise it will have a noticeable impact on the circular Hough transforms.

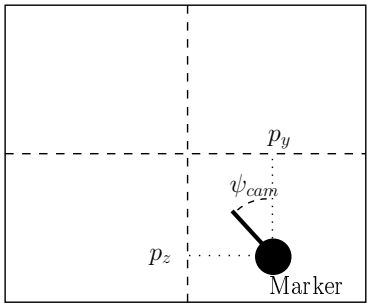

Figure 5. The marker with the yaw angle.

IV. Full State Slung Load Unscented Kalman Filter

The purpose of the slung load state estimator is to deliver estimates of the full helicopter and load state vector including position (${}^e\boldsymbol{R}_h \in \mathbb{R}^3, {}^e\boldsymbol{R}_l \in \mathbb{R}^3$), attitude (${}^e\boldsymbol{\theta}_h \in \mathbb{S}^3, {}^e\boldsymbol{\theta}_l \in \mathbb{S}^3$), velocity (${}^l\boldsymbol{v}_h \in \mathbb{R}^3, {}^l\boldsymbol{v}_l \in \mathbb{R}^3$) and rates (${}^e\boldsymbol{\omega}_h \in \mathbb{S}^3, {}^e\boldsymbol{\omega}_l \in \mathbb{S}^3$), where ^{e} denotes the earth fixed frame, ^{h} the helicopter fixed frame and ^{l} the load fixed frame.

IV.A. The Unscented Kalman Filter

An unscented Kalman filter approach is used as the architecture for both estimators. The UKF is a relative new approach to Kalman filtering. It was first proposed in [13] and later refined by [14] and in recent years it has been intensively researched for a wide range of estimation purposes. Its popularity is due to the fact that in theory the UKF yields estimates with higher precision compared to the conventional extended Kalman filter (EKF), as the UKF does not require first order linearisation of process and sensor models. However, this advantage is in many cases more theoretical that practical as modelling uncertainties are often more significant than linearisation errors [15]. Nevertheless, the possibility of using the nonlinear process and sensor models directly in the filter is a large advantage in many cases.

The core of the UKF is the Unscented Transform (UT) which is used to calculate mean and covariance values for a random variable through a deterministic sampling approach. The Unscented Transformation propagates the system state vector using a number $(2n+1)$ of carefully selected sample points, know as sigma points, $\mathcal{X}_{1,k-1}, \ldots, \mathcal{X}_{2n+1,k-1}$, where n is the number of states, through the non-linear model to evaluate the mean and covariance of the state estimate. For an in-depth description of the theory behind the UT see [16] and [17].

IV.B. IMU Driven Unscented Kalman Filter

This estimator is inspired by the IMU driven Kalman filter approach taken in much of the previous work described in section II. The general idea is to use the acceleration and rate input from two IMUs, one mounted on the helicopter and one mounted on the load, to drive the process model. To make sure that the constraints imposed by the wires are maintained, a simple technique is devised. A virtual sensor is introduced, which always measures the correct (not the actual) wire length and the sensor noise level in the filter for this sensor is set to a very low value. This ensures that the estimated states always obey the wire constraints. The filter includes estimation of biases on rates and accelerations for both IMUs. The IMU driven unscented Kalman filter is illustrated in figure 6.

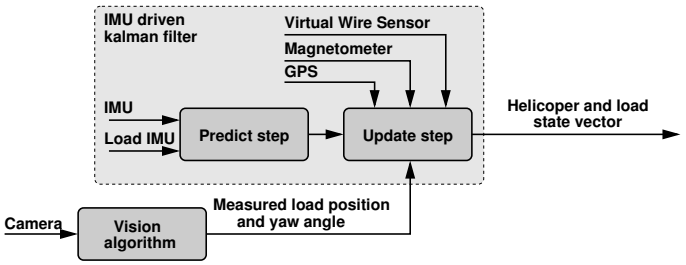

Figure 6. The architecture of the IMU driven unscented Kalman filter.

The state vector of the filter is specified as

$$\hat{\boldsymbol{x}} = \begin{bmatrix} {}^{e}\hat{\boldsymbol{R}}_{h} \\ {}^{e}\hat{\boldsymbol{\theta}}_{h} \\ {}^{e}\hat{\boldsymbol{R}}_{l} \\ {}^{e}\hat{\boldsymbol{\theta}}_{l} \\ {}^{h}\hat{\boldsymbol{v}}_{h} \\ {}^{l}\hat{\boldsymbol{v}}_{l} \\ {}^{h}\hat{\boldsymbol{B}}_{h} \\ {}^{l}\hat{\boldsymbol{B}}_{l} \end{bmatrix}_{30\times 1} \qquad {}^{b}\hat{\boldsymbol{B}}_{b} = \begin{bmatrix} {}^{b}\hat{\boldsymbol{a}}_{\mathrm{bias}b} \\ {}^{b}\hat{\boldsymbol{\omega}}_{\mathrm{bias}b} \end{bmatrix}_{6\times 1} \tag{5}$$

where $\hat{\boldsymbol{a}}_{\mathrm{bias}b}$ and $\hat{\boldsymbol{\omega}}_{\mathrm{bias}b}$ are the estimated acceleration and rate bias for the IMU mounted on body b. The measurement vector is defined as

$$\boldsymbol{z} = \begin{bmatrix} {}^{e}\tilde{\boldsymbol{R}}_{\mathrm{gps}} \\ {}^{e}\tilde{\boldsymbol{v}}_{\mathrm{gps}} \\ {}^{h}\tilde{\boldsymbol{M}}_{\mathrm{mag}} \\ {}^{h}\tilde{\boldsymbol{R}}_{\mathrm{cam}} \\ {}^{h}\tilde{\psi}_{\mathrm{cam}} \\ \tilde{\boldsymbol{W}}_{\mathrm{virt}} \end{bmatrix}_{(13+m)\times 1} \tag{6}$$

where ${}^{e}\tilde{\boldsymbol{R}}_{\mathrm{gps}}$ is the helicopter position measurement from the GPS, ${}^{e}\tilde{\boldsymbol{v}}_{\mathrm{gps}}$ is the helicopter velocity measurement from the GPS, ${}^{h}\tilde{\boldsymbol{M}}_{\mathrm{mag}}$ is the magnetic field measurement by the magnetometer, ${}^{h}\tilde{\boldsymbol{R}}_{\mathrm{cam}}$ is the load position measurement relative the helicopter from the vision system, and ${}^{h}\psi_{\mathrm{cam}}$ is the load yaw angle relative to the helicopter from the vision system. Finally, $\tilde{\boldsymbol{W}}_{\mathrm{virt}}$ is a vector consisting of the virtual measurements of the wire lengths, where m is the number of wires in the system.

IV.B.1. Process Model

The input to the process model is the accelerations and rates measured by the IMUs mounted on the helicopter and load. Before being used in the process model the raw measurements are corrected as

$$\tilde{\boldsymbol{a}}_{b,k} = \tilde{\boldsymbol{a}}_{\mathrm{IMU}b,k} - {}^{b}\hat{\boldsymbol{a}}_{\mathrm{bias}b,k-1} - \hat{\boldsymbol{T}}_{be,k-1}{}^{e}\boldsymbol{G}_{ref} \tag{7}$$

$$\tilde{\boldsymbol{\omega}}_{b,k} = \tilde{\boldsymbol{\omega}}_{\mathrm{IMU}b,k} - {}^{b}\hat{\boldsymbol{\omega}}_{\mathrm{bias}b,k-1} \tag{8}$$

for bias errors and for the acceleration also for the gravitational component. ${}^{e}\boldsymbol{G}_{ref}$ is the gravitational acceleration vector given in the earth fixed frame. The corrected measurements can then be used to calculate the elements of the derivative state vector as[18]

$${}^{e}\dot{\hat{\boldsymbol{R}}}_{b,k} = \hat{\boldsymbol{T}}_{eb,k-1}{}^{b}\hat{\boldsymbol{v}}_{b,k-1} \tag{9}$$

$${}^{e}\dot{\hat{\boldsymbol{\theta}}}_{b,k} = \hat{\boldsymbol{T}}_{\theta b,k-1}\tilde{\boldsymbol{\omega}}_{b,k} \tag{10}$$

$${}^{b}\dot{\hat{\boldsymbol{v}}}_{b,k} = \tilde{\boldsymbol{a}}_{b,k} - \tilde{\boldsymbol{\omega}}_{b,k} \times {}^{b}\hat{\boldsymbol{v}}_{b,k-1}\,. \tag{11}$$

The bias of MEMS sensors like those used in this application exhibit non-zero mean and non-stationary behaviour, which can be modelled as a random walk [10]. However, to track a random walk it suffices to use a constant process model

$$ {}^{b}\dot{\hat{\boldsymbol{B}}}_{b,k} = 0 \, . \tag{12} $$

The state vector defined in (5) is missing the angular velocity elements ${}^{h}\hat{\boldsymbol{\omega}}_{h}$ and ${}^{l}\hat{\boldsymbol{\omega}}_{l}$, but non-filtered estimates of these can be found from (8). It should be noted that any lever effect on the IMUs are neglected, as they are placed close to the centre of mass on both the helicopter and the load used in this study.

IV.B.2. Observation Models

The GPS outputs a measurement of the position of the helicopter in earth fixed frame using UTM coordinates. However, the GPS measurement on the helicopter position is not only dependent on the helicopter position, but also on the attitude of the helicopter as the GPS antenna is displaced from the CM as shown in figure 7. Furthermore, GPS measurements often exhibit quite high latencies, which can be compensated for by

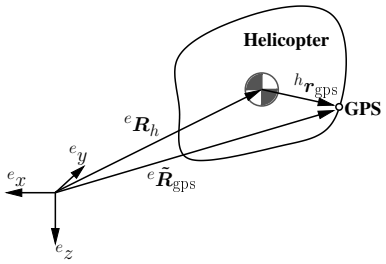

Figure 7. The displacement of the GPS from the CM.

simply incorporating a similar delay in the observation model. The GPS observation model is formulated as

$$ {}^{e}\hat{\boldsymbol{R}}_{\text{gps},k+\Delta gps} = {}^{e}\hat{\boldsymbol{R}}_{h,k} + \hat{\boldsymbol{T}}_{eh,k}\boldsymbol{r}_{\text{gps}} \, , \tag{13} $$

where Δgps is the latency of the GPS measurement. The GPS velocity measurement is modelled as the body fixed velocity compensated for the GPS offset using the bias corrected rate measurements and finally transformed into the earth fixed frame

$$ {}^{e}\hat{\boldsymbol{v}}_{\text{gps},k+\Delta gps} = \hat{\boldsymbol{T}}_{eh,k}({}^{b}\hat{\boldsymbol{v}}_{b,k} + \tilde{\boldsymbol{\omega}}_{b,k} \times \boldsymbol{r}_{\text{gps}}) \, . \tag{14} $$

The magnetometer output measurements of the magnetic field surrounding the helicopter, which is modelled simply as the earth fixed magnetic field reference (${}^{e}\boldsymbol{M}_{ref}$) rotated into the body frame

$$ {}^{h}\hat{\boldsymbol{M}}_{\text{mag},k} = \hat{\boldsymbol{T}}_{eh,k}{}^{e}\boldsymbol{M}_{ref} \, . \tag{15} $$

Part of the output of the vision system – as described in section III – is a unit vector (${}^{h}\tilde{\boldsymbol{R}}_{cam}$) pointing from the camera towards the marker on the load as shown on figure 8. This vector is dependent on the position of the helicopter and the load as well as the position of the camera on the helicopter (${}^{h}\boldsymbol{R}_{hc}$) and the position of the marker on the load (${}^{l}\boldsymbol{R}_{lm}$). The observation model, normalized to yield a unit vector, is formulated as

$$ {}^{h}\hat{\boldsymbol{R}}_{\text{cam},k+\Delta cam} = \frac{\hat{\boldsymbol{T}}_{he,k}({}^{e}\hat{\boldsymbol{R}}_{l,k} - {}^{e}\hat{\boldsymbol{R}}_{h,k} - \hat{\boldsymbol{T}}_{el,k}{}^{l}\boldsymbol{R}_{lm}) - {}^{h}\boldsymbol{R}_{hc}}{|\hat{\boldsymbol{T}}_{he,k}({}^{e}\hat{\boldsymbol{R}}_{l,k} - {}^{e}\hat{\boldsymbol{R}}_{h,k} - \hat{\boldsymbol{T}}_{el,k}{}^{l}\boldsymbol{R}_{lm}) - {}^{h}\boldsymbol{R}_{hc}|} \, , \tag{16} $$

where Δcam is the latency of the vision system.

The second part of the output from the vision system is a measurement of the yaw angle between the helicopter and the load. This is the angle between the straight line in the marker (denoted ${}^{l}\boldsymbol{r}_{m}$) and the z-axis of the camera. If considered in a small area around the round marker the visual output of the camera can be modelled as a plane with ${}^{h}\boldsymbol{R}_{cm}$ as normal. What the camera sees is then ${}^{l}\boldsymbol{r}_{m}$ projected onto this plane as shown in figure 9 where the projection is denoted ${}^{l}\boldsymbol{r}'_{m}$ The projection can be found as

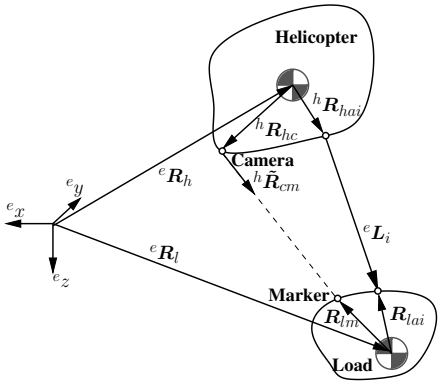

Figure 8. The geometric setup of position vision system model.

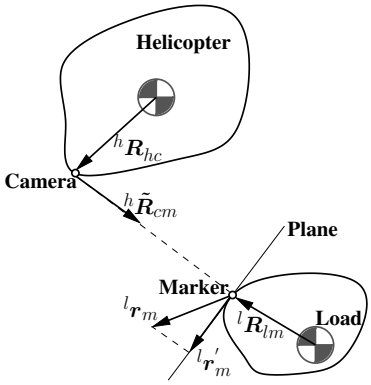

Figure 9. The setup of the yaw angle vision system angle.

$$ {}^{h}\boldsymbol{r}'_{m} = \hat{\boldsymbol{T}}_{he,k}\hat{\boldsymbol{T}}_{el,k}{}^{l}\boldsymbol{r}_{m} - (({}^{h}\hat{\boldsymbol{T}}_{he,k}\hat{\boldsymbol{T}}_{el,k}{}^{l}\boldsymbol{r}_{m}) \cdot {}^{l}\boldsymbol{R}_{cm})^{l}\boldsymbol{R}_{cm} \,, \tag{17} $$

which is calculated in helicopter frame as the camera is fixed to this frame. A new frame is defined, which coincides with the plane and has its third axis pointing along ${}^{h}\boldsymbol{R}_{cm}$ and its first axis aligned with the first axis of the helicopter frame. The Euler angles defining the rotation between the helicopter and the plane frame can be found as

$$ \phi_m = \arcsin({}^{h}R_{cm}(2)) \,, \qquad \theta_m = \arccos\left(\frac{{}^{h}R_{cm}(3)}{\cos(\phi_m)}\right) \,, \qquad \psi_m = 0 $$

where ${}^{h}R_{cm}(2)$ and ${}^{h}R_{cm}(3)$ denotes the second and third element of ${}^{h}\boldsymbol{R}_{cm}$. Using these Euler angles the rotation matrix $\boldsymbol{T}_{ph}$ can be formed and ${}^{p}\hat{\boldsymbol{r}}_{mp}$ can be calculated. Using the inner product the yaw angle vision system model can then be found as

$$ {}^{h}\hat{\psi}_{\text{cam},k+\Delta cam} = \arccos\left(\frac{{}^{p}\hat{r}_{mp,k}(1)}{|{}^{p}\hat{\boldsymbol{r}}_{mp,k}|}\right) . \tag{18} $$

where ${}^{p}\hat{r}_{mp,k}(1)$ is the first element of the vector ${}^{p}\hat{\boldsymbol{r}}_{mp,k}$.

The output of the virtual wire sensor is the nominal length of each of the m wires. By considering figure 8 where the i'th wire is shown it can be seen that the wire sensor can be modelled as

$$ \hat{\boldsymbol{W}}_{\text{virt},k} = \begin{bmatrix} |{}^{e}\hat{\boldsymbol{R}}_{h,k} + \hat{\boldsymbol{T}}_{eh,k}{}^{h}\boldsymbol{R}_{ha1} - {}^{e}\hat{\boldsymbol{R}}_{l,k} - \hat{\boldsymbol{T}}_{el,k}{}^{l}\boldsymbol{R}_{la1}| \\ \vdots \\ |{}^{e}\hat{\boldsymbol{R}}_{h,k} + \hat{\boldsymbol{T}}_{eh,k}{}^{h}\boldsymbol{R}_{ham} - {}^{e}\hat{\boldsymbol{R}}_{l,k} - \hat{\boldsymbol{T}}_{el,k}{}^{l}\boldsymbol{R}_{lam}| \end{bmatrix} , \tag{19} $$

where ${}^{h}\boldsymbol{R}_{hai}$ and ${}^{l}\boldsymbol{R}_{lai}$ points to the i'th attachment point on the helicopter and the load.

IV.C. Dynamic Process Model Unscented Kalman Filter

This approach uses a full dynamic aerodynamic and rigid body process model driven by control signals from the controller. As the filter uses the full slung load rigid body model is not mandatory to used the load IMU like it is in the IMU driven approach. It can be enabled or disabled depending on availability, but it should be noted that the roll and pitch dynamics of the load becomes weakly observable without the load IMU. Like with the IMU driven approach the filter includes estimates of biases on rates and accelerations and it furthermore includes estimation of external wind influences which acts as bias in the dynamical model. The model based approach is illustrated in figure 10

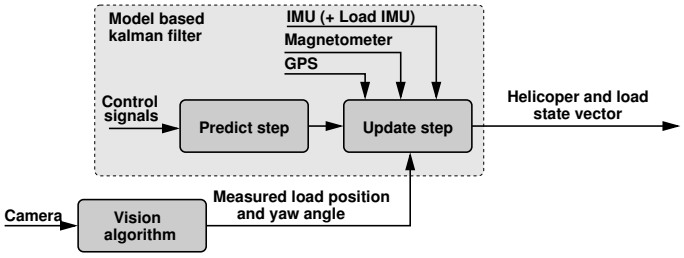

Figure 10. The architecture of the dynamic model based unscented Kalman filter.

The state and measurement vectors for the model based approach are specified as

$$\hat{\boldsymbol{x}} = \begin{bmatrix} {}^{e}\hat{\boldsymbol{R}}_{h} \\ {}^{e}\hat{\boldsymbol{\theta}}_{h} \\ {}^{e}\hat{\boldsymbol{R}}_{l} \\ {}^{e}\hat{\boldsymbol{\theta}}_{l} \\ {}^{h}\hat{\boldsymbol{v}}_{h} \\ {}^{h}\hat{\boldsymbol{\omega}}_{h} \\ {}^{l}\hat{\boldsymbol{v}}_{l} \\ {}^{l}\hat{\boldsymbol{\omega}}_{l} \\ {}^{e}\hat{\boldsymbol{v}}_{w} \\ {}^{h}\hat{\boldsymbol{B}}_{h} \\ {}^{l}\hat{\boldsymbol{B}}_{l} \end{bmatrix}_{39\times 1} \qquad \boldsymbol{z} = \begin{bmatrix} {}^{e}\tilde{\boldsymbol{R}}_{\text{gps}} \\ {}^{e}\tilde{\boldsymbol{v}}_{\text{gps}} \\ {}^{h}\tilde{\boldsymbol{M}}_{\text{mag}} \\ {}^{h}\tilde{\boldsymbol{\omega}}_{\text{IMU}h} \\ {}^{h}\tilde{\boldsymbol{a}}_{\text{IMU}h} \\ {}^{l}\tilde{\boldsymbol{\omega}}_{\text{IMU}l} \\ {}^{l}\tilde{\boldsymbol{a}}_{\text{IMU}l} \\ {}^{h}\tilde{\boldsymbol{R}}_{\text{cam}} \\ {}^{h}\tilde{\psi}_{\text{cam}} \\ \tilde{\boldsymbol{W}}_{\text{virt}} \end{bmatrix}_{(25+m)\times 1} \tag{20}$$

where ${}^{e}\hat{\boldsymbol{v}}_{w}$ is the external wind in earth fixed frame.

As mentioned earlier it is possible to reduce the state vector to 33 elements as the 6 bias states for the load IMU can be eliminated when this sensor is not available. This also reduces the measurement vector with the associated 6 states, but by removing the IMU on the load observability is affected. When considering observability for the estimators there are no sensors that measure the roll and pitch attitude of the load directly. If the IMU on the load is used, it provides roll and pitch rate information and the accelerometers provide some information on the the load roll and pitch attitude through the gravity. However, it is possible to achieve full observability through the choice of suspension type. If suspension type (b) from figure 1 is used the pitch of the load is directly coupled with the pitch of the helicopter, but the roll is uncoupled. If type (c) or (d) is chosen both roll and pitch of the load is linked to the helicopter and these becomes observable though the the helicopter attitude and the load position.

IV.C.1. Process Model

The process model for the model based estimator consists of an aerodynamical helicopter model and a generic two-body rigid body model. The helicopter model is based on the principles presented in [19] and [20], but it is modelled entirely as steady state which means that only the rigid body states are left. This is due to the fact that actuator dynamics, inflow dynamics, and flapping dynamics are of little interest from a control point of view and furthermore these states are quite a lot faster than what is feasible to estimate considering the available computational resources.

Flapping is calculated for both the stabiliser bar and the main rotor and it is derived using blade element analysis and solved as steady state. Forces and torques for the main and tail rotor also derived using blade element analysis. An uniform inflow model is used which is derived momentum theory is used and it is solved using an analytical solution scheme.

The rigid body model is derived using a redundant coordinate formulation based on Gauss' Principle of Least Constraint using the Udwadia-Kalaba equation[21] and can be used to model all body to body slung load suspension types. The rigid body model is simple and intuitive, and due to the redundant coordinate formulation it is possible to change suspension system on the fly. For a presentation of the rigid body model see [18].

The bias model is the same as the one presented under the IMU driven process model in (12) and the wind is likewise modelled as a stationary process

$$ {}^{e}\dot{\hat{\boldsymbol{v}}}_{w,k} = 0 \,. \tag{21} $$

IV.C.2. Observation Models

The observation models for the GPS, the magnetometer, the virtual wire sensor, and the vision system are the same as the ones presented under the IMU driven filter. However, the IMUs are now present as sensors and therefore needs observation models, which are simply rewrites of (7) and (8)

$$ \hat{\boldsymbol{a}}_{\text{IMU}b,k} = \hat{\boldsymbol{a}}_{b,k} + {}^{b}\hat{\boldsymbol{a}}_{\text{bias}b,k} + \hat{\boldsymbol{T}}_{be,k}\,{}^{e}\boldsymbol{G}_{ref} \tag{22} $$

$$ \hat{\boldsymbol{\omega}}_{\text{IMU}b,k} = \hat{\boldsymbol{\omega}}_{b,k} + {}^{b}\hat{\boldsymbol{\omega}}_{\text{bias}b,k} \,, \tag{23} $$

$\hat{\boldsymbol{a}}_{b,k}$ is not part of the state vector of the system, but is instead extracted from the process model prediction step during the propagation of the first sigma point.

IV.D. Implementations Considerations

In the IMU driven filter the process model is propagated using a standard forward Euler approach, whereas in the model based filter it is propagated using a second order Runge-Kutta approach. This is because the solution of the redundant coordinate rigid body model benefits greatly from the added numerical precision of the second order Runge-Kutta as compared to the forward Euler. Both filters are run at 50 Hz, which is adequate for estimation of the rigid body dynamics.

Some of the sensors available in the system are unable to deliver output at the filter execution frequency. The GPS, for instance, is capable of an output rate of 20 Hz and the vision system can deliver new measurements at a rate of about 15 Hz. In order to deal with this, a simple solution is used – when a measurement is not available, the column in the Kalman gain corresponding to the missing measurement is simply set equal to 0. Thereby, the missing data is not allowed to influence on the prediction of the state vector. This is in practice done by comparing one sample time old sensor measurements with the new ones and if there is no difference, the sensor is disabled. This is a simple approach, which relies on a certain noise level on all sensors and it automatically deals with some sensor fault.

V. State Dependent Separation

When using the unscented Kalman filter an important issue is the computational demands of the prediction step – the UKF can be come very computational demanding when used in connection with a complex model with many states like the one used in the model based filter here. As mentioned earlier the UKF actually requires $2n+1$ calls of the model which in the IMU driven case yields 61 calls of the model. However, in the model based case this becomes 79 calls from the UKF and for each call the model is executed twice in the second order Runge-Kutta with yields a total of 158 model calls for each time step. As the filter is run at 50 Hz and as the model is quite complex, the computational burden is high. Therefore a simple method for speeding up the model propagation is devised.

For the dynamical helicopter slung load model used in this research it is possible to make a separation into a sequential set of parts that can be calculated one after another. Indeed this is possible for a wide range of dynamical models. This is interesting when the model is used in the unscented Kalman filter where the sigma points that are propagated contains perturbations on one state at a time with respect to the mean state vector (which is equal to the first sigma point).

Assume that a n'th state in the state vector, which is propagated with sigma point $n+1$ and $2n+1$ as

$$\boldsymbol{\chi}_0 = \begin{bmatrix} x_1 \\ x_2 \\ \vdots \\ x_n \end{bmatrix}, \quad \boldsymbol{\chi}_{n+1} = \begin{bmatrix} x_1 \\ x_2 \\ \vdots \\ x_n + \delta_s \end{bmatrix}, \quad \boldsymbol{\chi}_{2n+1} = \begin{bmatrix} x_1 \\ x_2 \\ \vdots \\ x_n - \delta_s \end{bmatrix},$$

where δ_s is the sigma point perturbation term, is only used in the last part of the model. This means that the model can be separated into two parts, one that is independent of x_n

$$\boldsymbol{y}_1 = \boldsymbol{f}_1(\boldsymbol{u}, x_1, x_2, \ldots, x_{n-1}),$$

and one that is dependent on x_n, the output of the first part and possibly the other states as well

$$\boldsymbol{y}_2 = \boldsymbol{f}_2(\boldsymbol{y}_1, \boldsymbol{u}, x_1, x_2, \ldots, x_n),$$

where $\boldsymbol{y}_2$ is the final output of the model. This separation can then be used in the unscented Kalman filter where the output of $\boldsymbol{f}_1$ from the first sigma point ($\boldsymbol{y}_{1,1}$) is reused in the calculation of $\boldsymbol{f}_2$ for sigma point $n+1$ and $2n+1$ and thereby saving two calculations of $\boldsymbol{f}_1$. This is illustrated in figure 11.

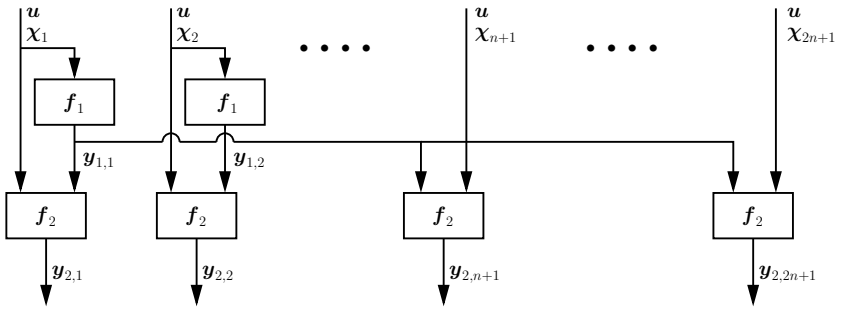

Figure 11. The state dependent separation principle used in the propagation of the sigma points.

This principle can be used with great success on the helicopter and slung load dynamical model where the entire aerodynamical helicopter model only depends on the helicopter velocities and therefore only needs to be calculated for 6 out of 24 rigid body states. Furthermore, the helicopter and slung load model is completely independent of the IMU bias states. This means that out of the 158 total calls to the model only 62 full calls are needed using this principle. Another 48 partial calls of the model, where only the rigid body part of the model is call, are needed. Finally, 48 calls where it is unnecessary to call the helicopter slung load model at all and only the simple bias model is used.

VI. Test and Comparison

The two estimators are tested on a simple trajectory in close loop using a optimal state feedback controller. The sensors are modelled using realistic noise, quantisation, and delays. In the case of the IMU on the helicopter, the noise levels are quite high due to vibrations induced by the engine and rotors. The GPS using EGNOS has a horisontal accuracy of approximately 1 m, which is modelled as white noise together with random walk. External wind is modelled as a constant vector overlayed with smaller sinusoids. Biases are modelled as constants overlayed with random walks. The parameters of the model used in the model based filter has been changed with 10% with respect to the model used to simulate the system, which helps ensuring a realistic simulation. A 4 m dual wire suspension, like the one shown in figure 1 (b), is chosen for the test.

The trajectory is a S-like pattern starting and stopping in hover. In figure 12 the trajectory flow using the IMU driven filter is shown. The estimation errors for the IMU driven filter is shown in figure 13. It is capable of tracking the position of the helicopter and the load within 0.2 m, the attitude within 0.05 rad, and velocity within 0.5 m/s after the filter converges. The filter convergence is evident from the error on the biases, the biases on the gyros converges quickly after only a few seconds, while the biases on the accelerometers takes

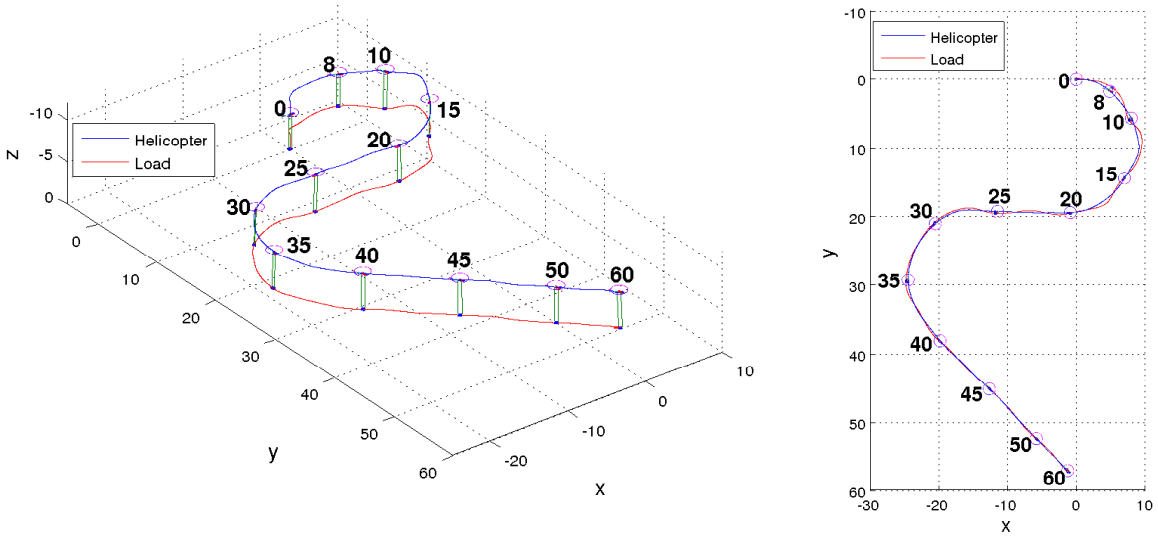

Figure 12. 3D plot of the trajectory flow with the IMU driven filter shown in perspective and from the top with timeline.

slightly longer to converge. As mentioned earlier the rate estimates are simply bias compensated gyro measurements and the vibration noise from the helicopter is evident on the rate estimation error. The wire length error is less that 1 mm.

The trajectory flow with the with the model based filter is shown in figure 14. When comparing the estimation errors for the model based filter in figure 15 with errors for the IMU driven filter, the results are similar if slightly better for the model based filter. However, some differences stand out. The vibrational noise, that was very evident on the helicopter rate estimate with the IMU driven filter, is reduced significantly. The bias estimation for the load exhibits a large deviation on the z-axis due to numerical inprecisions in the initialization of the rigid body model, but it converges quickly. The wind estimates, which are avilable in the model based filter, is shown and follows the real wind quite well.

The execution time for the filters is shown in table 1, which compares the IMU driven with the full model based solution. For the model based solution the result with and without using the state dependent seperation is shown. The execution time is measured in % of the avilable computational time when running

Estimator	Execution time, % of avilable time
IMU driven filter	5.1
Model based filter (optimized)	30.5
Model based filter	46.4

Table 1. Execution time comparison for the IMU driven filter, the optimized model based filter and the standard model based filter.

the system at 50 Hz on the 1.8 GHz onboard computer. In other words, when the IMU driven filter uses 5.1% of the computational resources there is 94.9% time left for controllers, supervisiors etc. As it can be seen the model based filter uses a substantial percentage of the available resources, but this can be reduced by approximately 1/3 by using the state seperation priciple presented earlier.

VII. Conclusion

In this paper a state estimator for a helicopter slung load system was presented. Two different approaches was investigated: A kinematic model and a full model based filter, both based on the unscented Kalman filter. The kinematic model filter was based on a simple IMU driven model, while the full model based filter used a complex dynamic model using advanced aerodynamic and rigid body equations. A standard sensor

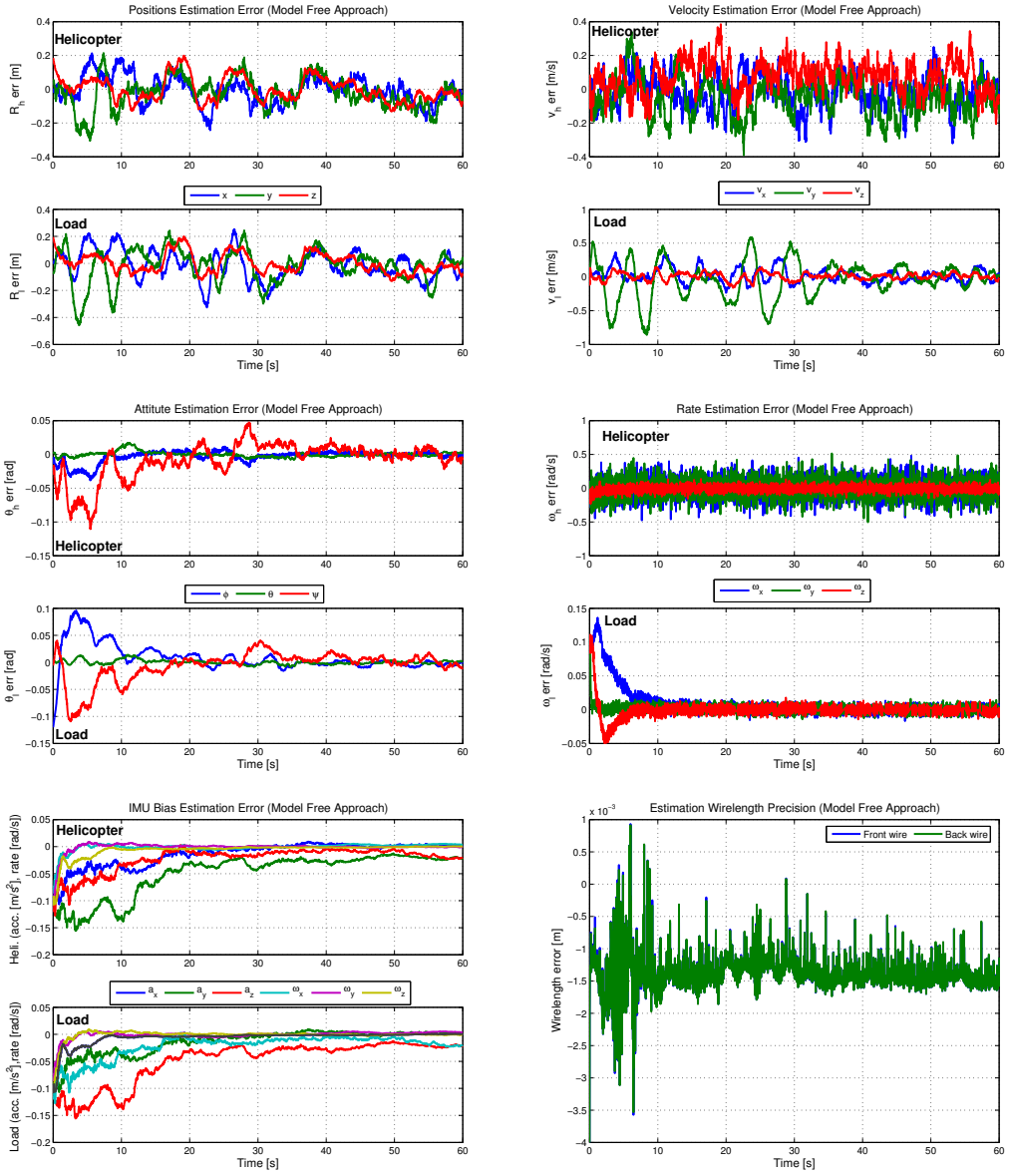

Figure 13. Estimation errors using the IMU driven filter.

setup was used for the helicopter including GPS, magnetometer, and IMU. A vison based system was used to detect attitude and position of the load and an IMU was mounted on the load. To reduce the computational requirements for the estimators a simple principle was devised, which ensured that only the necessary parts of the process model was executed in the unscented Kalman filter.

The filters was tested through simulation in close loop and the controller was capable of tracking the specified trajectory using both filters. It can therefore be concluded that both filters performs satisfactory. The estimator errors for the two filters was compared and the full model based filter was found to perform somewhat better that the filter based on the kinematic model, but at the expense of a rather high computational burden.

References

[1]Prabhakar, A., *Stability of a Helicopter Carrying an Underslung Load*, Vertica, Vol. 2, pp 121-143, 1978.

[2]Ronen, T., Bryson, A. E., and Hindson, W. S., *Dynamics of a Helicopter with a Sling Load*, AIAA Atmospheric Flight Mechanics Conference, 1986, AIAA number 86-2288.

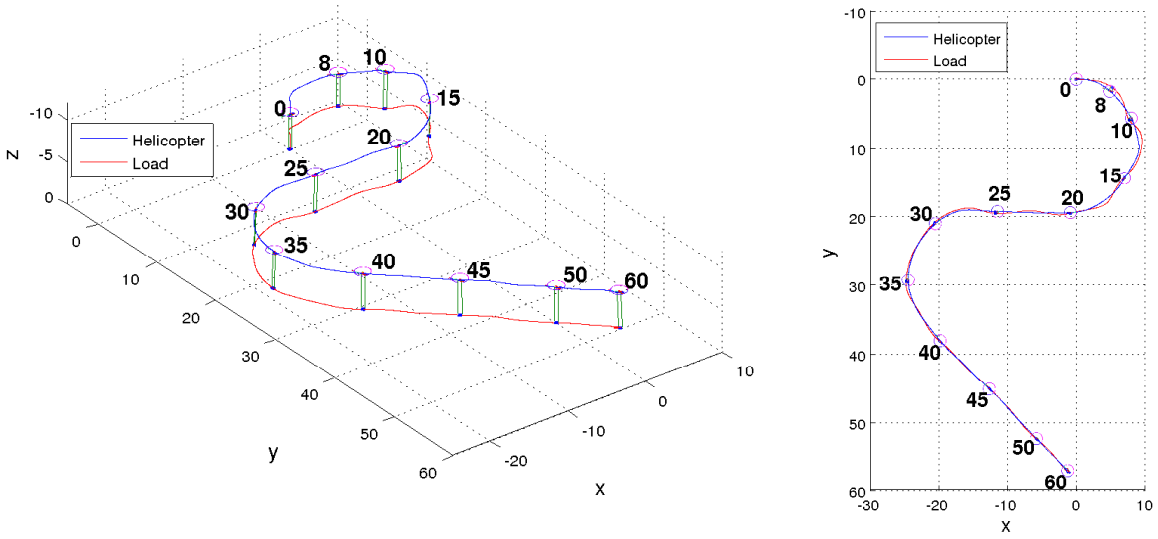

Figure 14. 3D plot of the trajectory flow with the model based filter shown in perspective and from the top with timeline.

[3]Human Rights Watch, *Landmine Monitor Report*, Landmine Monitor Core Group, 2005.

[4]Rock, S. M., Frew, E. W., Jones, H., LeMaster, E. A., and Woodley, B. R., *Combined CDGPS and Vision-Based Control of a Small Autonomous Helicopter*, Proceedings of the American Control Conference, pp. 694-698, 1998.

[5]Baerveldt, A.-J. and Klang, R., *A Low-cost and Low-weight Attitude Estimation System for an Autonomous Helicopter*, IEEE International Conference on Inteligent Engineering Systmes, pp. 391-395, 1997.

[6]Jun, M., Roumeliotis, S. I., and Sukhatme, G. S., *State Estimation of an Autonomous Helicopter Using Kalman Filtering*, International Conference on Intelligent Robots and Systems, 1999.

[7]Gavrilets, V., Shterenberg, A., Dahleh, M. A., and Feron, E., *Avionics System For A Small Unmanned Helicopter Performing Agressive Maneuvers*, IEEE Aerospace and Electronic Systems Magazine, 2001.

[8]Saripoalli, S., Roberts, J. M., Corke, P. I., and Buskey, G., *A Tale of Two Helicopters*,
Proceedings of IEEE/RSJ International Conference on Intelligent Robots and Systems, pp. 805-810, 2003.

[9]Musial, M., Deeg, C., Remuss, V., and Hommel, G., *Orientation Sensing for Helicopter UAVs under Strict Resource Constraints*, First European Micro Air Vehicle Conference, 2004.

[10]van der Merwe, R., Wan, E., Julier, S., Bogdanov, A., Harvey, G., and Hunt, J., *Sigma-Point Kalman Filters for Nonlinear Estimation and Sensor Fusion: Applications to Integrated Navigation*, AIAA Guidance Navigation & Control Conference, 2004.

[11]Matsuoka, M., Surya Singh, A. C., Coates, A., Ng, A. Y., and Thrun, S., *Autonomous Helicopter Tracking and Localization Using a Self-Calibrating Camera Array*, Proceedings of the Fifth International Conference on Field Service Robotics, 2005.

[12]Gupta, N. K. and Arthur E. Bryson, J., *Near-Hover Control of a Helicopter with a Hanging Load*, Journal of Aircraft, Vol. 13, No. 3, pp. 217-222, 1976.

[13]Julier, S. J. and Uhlmann, J. K., *A New Extension of the Kalman Filter to Nonlinear Systems*,
University of Oxford, 1997.

[14]Wan, E. A. and van der Merwe, R., *The Unscented Kalman Filter for Nonlienar Estimation*,
Oregon Graduate Institute of Science and Technology, 2000.

[15]Bisgaard, M., Vinther, D., Østergaard, K., Bendtsen, J., and Izadi-Zamanabadi, R., *Sensor Fusion and Model Verification for a Mobile Robot*, 16th IASTED International Conference on Modelling and Simulation, 2005.

[16]Julier, S. J. and Uhlmann, J. K., *A General Method for Approximating Nonlinear Transformations of Probability Distributions*,
Technical report, Dept. of Engineering Science, University of Oxford, 1996.

[17]Julier, S. J. and Uhlmann, J. K., *A Consistent, Debiased Method for Converting Between Polar and Cartesian Coordiante Systems*,
In Proceedings of AeroSense, The 11th International Symposium on Aerospace/Defense Sensing, Simulation and Control Conference, 1997.

[18]Bisgaard, M., la Cour-Harbo, A., and Bendtsen, J. D., *Modelling of a Generic Slung Load System*, AIAA Modelling and Simulation Conference, 2006.

[19]Talbot, P. D., Tinling, B. E., Decker, W. A., and Chen, R. T. N., *A Mathematical Model of a Single Main Rotor Helicopter for Piloted Simulation*, Nasa, 1982.

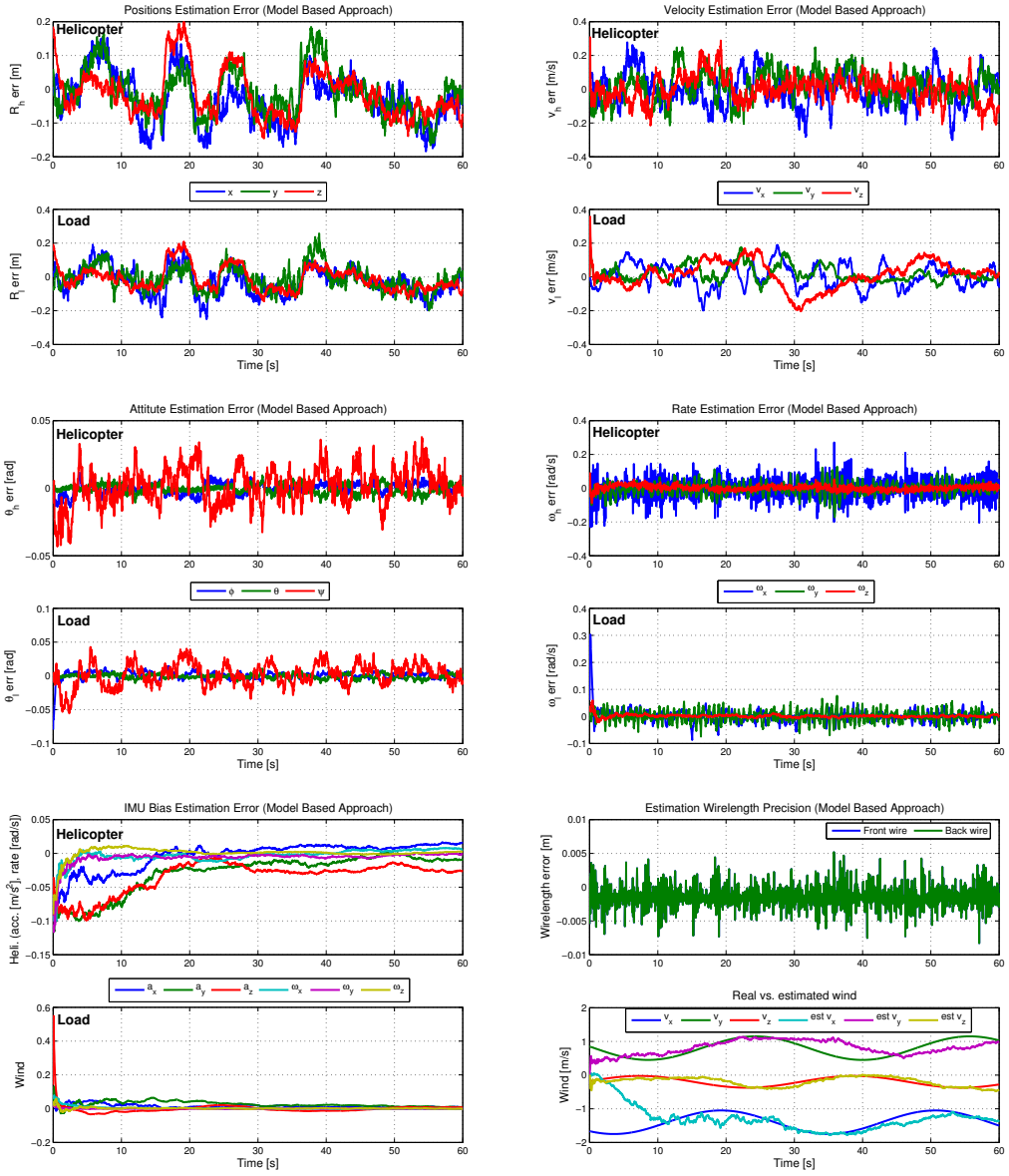

Figure 15. Estimation errors using the model based filter.

[20]Civita, M. L., *Integrated Modeling and Robust Control for Full-Envelope Flight of Robotic Helicopters*, Carnegie Mellon University, 2002, PhD Thesis.

[21]Udwadia, F. E. and Kalaba, R. E., *A new perspective on constrained motion*, In Proceedings: Mathematical and Physical Sciences, Vol 439, Issue 1906, pp 407-410, 1992.